# Anisotropic spatially heterogeneous dynamics on the $\alpha$ and $\beta$ relaxation time scales studied via a four-point correlation function

Elijah Flenner and Grzegorz Szamel

*Department of Chemistry, Colorado State University, Fort Collins, Colorado 80523, USA*

We examine the anisotropy of a four-point correlation function $G_4(\vec{k},\vec{r};t)$ and its associated structure factor $S_4(\vec{k},\vec{q};t)$ calculated using Brownian dynamics computer simulations of a model glass forming system. These correlation functions measure the spatial correlations of the relaxation of different particles. We examine the time and temperature dependences of the anisotropy in both functions. We find that the anisotropy is strongest at nearest-neighbor distances at time scales corresponding to the peak of the non-Gaussian parameter $\alpha_2(t)$ $=3\langle \delta r^4(t)\rangle/[5\langle \delta r^2(t)\rangle^2]-1$ but is still pronounced around the $\alpha$ relaxation time. We find that the structure factor $S_4(\vec{k},\vec{q};t)$ is anisotropic even for the lowest wave vector accessible in our simulation, suggesting that our system (and other systems commonly used in computer simulations) may be too small to extract the $\vec{q}\rightarrow 0$ limit of the structure factor. We find that the determination of a dynamic correlation length from $S_4(\vec{k},\vec{q};t)$ is influenced by the anisotropy. We extract an effective anisotropic dynamic correlation length from the small $q$ behavior of $S_4(\vec{k},\vec{q};t)$.

## I. INTRODUCTION

It is now generally accepted that upon approaching the glass transition, the liquid's dynamics are becoming increasingly heterogeneous [1–3]. However, the details of the spatial and temporal characteristics of dynamic heterogeneities are still being debated. In particular, the connection between heterogeneous dynamics and a growing dynamic correlation length has been the topic of many simulations [4–11] and a few experimental studies [12–14]. Four-point correlation functions have been introduced to facilitate the quantitative description of heterogeneous dynamics. The analysis of the spatial decay of these correlation functions was used to extract a dynamic correlation length. Recently, the mode-coupling theory has been extended and a theoretical treatment of four-point correlation functions is starting to emerge [6,12,15–18]. However, in most simulation studies and in some theoretical treatments, these four-point correlation functions have been assumed to be isotropic or they are isotropic by design.

Researchers have noticed anisotropy in the correlated motion of particles on the $\beta$ relaxation time scale, and recently this anisotropic motion has also been reported on the $\alpha$ relaxation time scale [19]. Doliwa and Heuer [20,21] reported anisotropic-correlated motion in a hard-sphere system on the $\beta$ relaxation time scale. Anisotropic motion has also been extensively studied by Donati *et al.* [8] and Gebremichael *et al.* [22] who described the motion of "mobile" particles as "stringlike," with mobile particles following each other in one dimensional "strings." Weeks and Weitz [23] reported anisotropic dynamics associated with the break down of the "cage" surrounding a particle. They found that the correlations of the particle's displacements depend on the initial separation of the particles. While particles that start at a separation corresponding to the first peak of the pair-correlation function are most likely to move in the same direction, particles that start at a separation corresponding to the first minimum are more likely to initially move in opposite directions.

In view of the experimental and simulational evidence for anisotropic correlations of particle's displacements, it should not be a surprise that four-point correlation functions designed to study these dynamics can also be anisotropic. However, this anisotropy is normally studied for times less than the $\alpha$ relaxation time; thus it is uncertain if understanding this anisotropy is important for the structural relaxation of the liquid. Previously [19] we reported on a four-point correlation function that is anisotropic on the $\alpha$ relaxation time scale as well as the $\beta$ relaxation time scale for a model glass forming liquid. Since the spatial decay of this correlation function can be used to determine a dynamic length scale, the anisotropy introduces a complication in determining this length scale.

In this paper we expand on previous work [19]. In particular, here we examine the temperature dependence of the anisotropy of a four-point correlation function in more detail than in Ref. [19], and we present an algorithm to determine an anisotropic correlation length. After describing the simulation in Sec. II, we explore the anisotropic-correlated dynamics by examining a four-point correlation function $G_4(\vec{k},\vec{r};t)$ (Sec. III) and the associated structure factor $S_4(\vec{k},\vec{q};t)$ (Sec. IV). We examine the anisotropy at around nearest-neighbor distances, which corresponds to the local rearrangement of particles and its cage and at large distances. Our conclusions from the analysis of the four-point correlation function are similar to those of Weeks and Weitz [23] about the breakup of the cage surrounding a particle. We examine how the anisotropy influences the determination of a growing length scale accompanying the glass transition and evaluate an effective anisotropic correlation length. We find that the dynamic correlation length is larger in the direction of motion of a particle than in the direction perpendicular to that motion. A similar result was obtained by Doliwa and Heuer [20] using a different correlation function. We finish with a discussion of the results in Sec. V.

## II. SIMULATION

We performed Brownian dynamics simulations of an 80:20 binary mixture of 1000 particles introduced by Kob and Andersen [24,25]. The interaction potential is $V_{\alpha\beta}(r) = 4\epsilon_{\alpha\beta}[(\sigma_{\alpha\beta}/r)^{12} - (\sigma_{\alpha\beta}/r)^6]$ where $\alpha$, $\beta \in \{A,B\}$, $\epsilon_{AA}=1.0$, $\epsilon_{AB}=1.5$, $\epsilon_{BB}=0.5$, $\sigma_{AA}=1.0$, $\sigma_{AB}=0.8$, and $\sigma_{BB}=0.88$ and the interaction potential is cut at 2.5 $\sigma_{\alpha\beta}$. Periodic boundary conditions were used with a box length of 9.4 $\sigma_{AA}$. The equation of motion for the position of particle $i$ is

$$\dot{\vec{r}}_i = \frac{1}{\xi_0}\vec{F}_i(t) + \vec{\eta}_i(t), \qquad (1)$$

where $\xi_0=1.0$ is the friction coefficient of an isolated particle and the force acting on a particle $i$ is

$$\vec{F}_i = -\nabla_i \sum_{n\neq i} V_{\alpha\beta}(|\vec{r}_i - \vec{r}_n|), \qquad (2)$$

with $\nabla_i$ being the gradient operator with respect to $\vec{r}_i$. The random force $\vec{\eta}(t)$ satisfies the fluctuation dissipation relation

$$\langle \vec{\eta}_i(t)\,\vec{\eta}_j(t')\rangle = 2D_0\delta_{ij}\mathbf{1}, \qquad (3)$$

where $D_0=k_BT/\xi_0$, $k_B$ is the Boltzmann's constant, and $\mathbf{1}$ is the unit tensor. The results are presented in terms of reduced units with $\sigma_{AA}$, $\epsilon_{AA}/k_B$, and $\sigma_{AA}^2\xi_0/\epsilon_{AA}$ being the units of length, energy, and time, respectively. Since the equation of motion allows for diffusion of the center of mass, all results are presented relative to the center of mass.

We present results for temperatures $T=0.45$, 0.47, 0.5, 0.55, 0.6, 0.8, 0.9, and 1.0. The onset of supercooling is around $T=1.0$ and we use $T_c=0.435$ as the mode-coupling temperature. As a means to expand the temperature scale, we will plot some quantities versus $\epsilon=(T-T_c)/T_c$. The equation of motion was integrated using a Heun algorithm with a small time step of $5\times10^{-5}$. We ran an equilibration run that was at least half as long as a production run and four production runs at each temperature. The results are an average over the production runs. We present results only for the larger and more abundant $A$ particles. We define the $\alpha$ relaxation time $\tau_\alpha$ as $F_s(\vec{k};\tau_\alpha)=e^{-1}$ for a wave vector around the first peak of the partial static structure factor for the $A$ particles, which corresponds to $|\vec{k}|=7.25$.

## III. FOUR-POINT CORRELATION FUNCTION $G_4(\vec{k},\vec{r};t)$

### A. Definition and connection with overlap correlations

We study a four-point correlation function that measures the spatial and temporal correlations between the relaxation of different particles. Consider the function

$$\hat{F}_n(\vec{k};t) = e^{-i\vec{k}\cdot[\vec{r}_n(t)-\vec{r}_n(0)]}, \qquad (4)$$

where $\vec{r}_n(t)$ is the position of particle $n$ at a time $t$. The ensemble average of $\hat{F}_n(\vec{k};t)$ is the self-intermediate scattering function $F_s(k;t)$, thus we will term $\hat{F}_n(\vec{k};t)$ as the microscopic self-intermediate scattering function. The four-point correlation function

$$G_4(\vec{k},\vec{r};t) = \frac{V}{N^2}\sum_{n\neq m}\langle \hat{F}_n(\vec{k};t)\hat{F}_m(-\vec{k};t)\delta[\vec{r}-\vec{r}_{nm}(0)]\rangle \quad (5)$$

measures the correlations between the microscopic self-intermediate scattering function at time $t$, pertaining to particles that are separated by a vector $\vec{r}$ at the initial time. In Eq. (5) $\vec{r}_{nm}=\vec{r}_n-\vec{r}_m$, $V$ is the volume, and $N$ is the number of particles. Notice that $G_4(\vec{k},\vec{r};0)=g(r)$ where $g(r)$ is the pair-correlation function. In this work, we choose $|\vec{k}|$ to have the same value as the one that determines the $\alpha$ relaxation time, i.e., $|\vec{k}|$ is located around the first peak of the partial static structure factor for the $A$ particles, $|\vec{k}|=7.25$.

It should be noted that $G_4(\vec{k},\vec{r};t)$ is, in general, complex. Its real and imaginary parts can be written in the following form:

$$\mathrm{Re}[G_4(\vec{k},\vec{r};t)]$$
$$= \frac{V}{N^2}\sum_{n\neq m}\langle\cos\{\vec{k}\cdot[\vec{r}_{nm}(t)-\vec{r}_{nm}(0)]\}\delta[\vec{r}-\vec{r}_{nm}(0)]\rangle,$$
$$(6)$$

$$\mathrm{Im}[G_4(\vec{k},\vec{r};t)]$$
$$= -\frac{V}{N^2}\sum_{n\neq m}\langle\sin\{\vec{k}\cdot[\vec{r}_{nm}(t)-\vec{r}_{nm}(0)]\}\delta[\vec{r}-\vec{r}_{nm}(0)]\rangle.$$
$$(7)$$

Equations (7) and (8) show that particles which are getting closer together or farther apart along the direction of vector $\vec{k}$ (i.e., are moving in the opposite direction or in the same direction along $\vec{k}$) make the same contribution to the real part of $G_4(\vec{k},\vec{r};t)$ but opposite contributions to its imaginary part. In particular, particles moving farther apart along the direction of vector $\vec{k}$ make a negative contribution to the imaginary part of $G_4(\vec{k},\vec{r};t)$.

In several other simulational and experimental studies [9,10,26,27], four-point correlation functions involving single-particle overlaps rather than the microscopic self-intermediate scattering functions were investigated. For example, Lacevic et al. [9] used the following function [28]:

$$g_4^{ol}(r;t) = \frac{V}{N^2}\sum_{n\neq m}\langle w_n(a;t)w_m(a;t)\delta[\vec{r}-\vec{r}_{nm}(0)]\rangle, \quad (8)$$

where $w_n(a;t)$ is the overlap function pertaining to particle $n$,

$$w_n(a;t) = \theta(a-|\vec{r}_n(t)-\vec{r}_n(0)|). \qquad (9)$$

We would like to point out that $g_4(r;t)$ can be expressed in terms of functions which are generalizations of our $G_4(\vec{k},\vec{r};t)$,

$$g_4^{ol}(r;t) = \int \frac{d\vec{k}_1 d\vec{k}_2}{(2\pi)^6} f(k_1;a)f(k_2;a)\mathcal{G}_4(\vec{k}_1,\vec{k}_2,\vec{r};t), \quad (10)$$

where $\mathcal{G}_4(\vec{k}_1,\vec{k}_2,\vec{r};t)$ is defined as the correlation function of the microscopic self-intermediate scattering functions at time $t$ and calculated for different wave vectors,
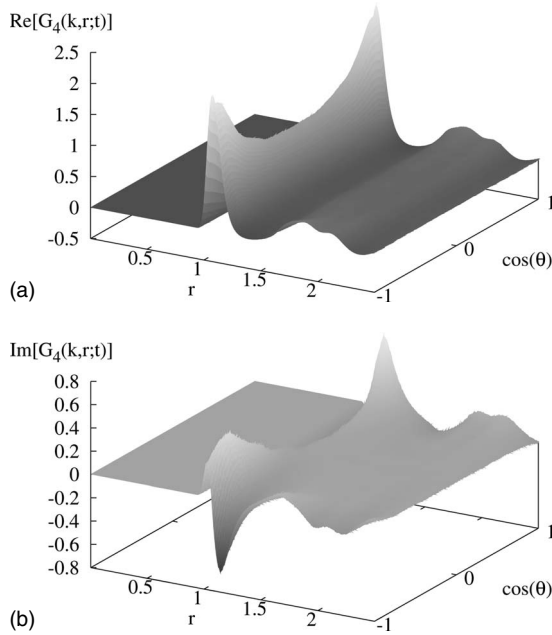
FIG. 1. (a) The real part of the correlation function $G_4(\vec{k}, \vec{r}; \tau_\alpha)$ and (b) the imaginary part of $G_4(\vec{k}, \vec{r}; \tau_\alpha)$ for $T=0.45$ calculated at the $\alpha$ relaxation time.

$$\mathcal{G}_4(\vec{k}_1, \vec{k}_2, \vec{r}; t) = \frac{V}{N^2} \sum_{n \neq m} \langle \hat{F}_n(\vec{k}_1; t) \hat{F}_m(\vec{k}_2; t) \delta[\vec{r} - \vec{r}_{nm}(0)] \rangle,$$

(11)

and $f(k; a) = 4\pi a^2 j_1(ka)/k$ with $j_1$ denoting a spherical Bessel function of the first kind.

The present work is mostly concerned with the anisotropic nature of dynamic heterogeneities, which can be monitored using the four-point correlation function given by Eq. (5). In this context we would like to emphasize that, in principle, the more general function (11) is also anisotropic. However, any trace of this anisotropy is lost after the integration over wave vectors $\vec{k}_1$ and $\vec{k}_2$ and thus the overlap correlation function (8) is—by construction—isotropic.

### B. Anisotropy of $G_4(\vec{k}, \vec{r}; t)$

Since the functions $\hat{F}_n(\vec{k}; t)$ are sensitive to displacements of particles along the direction of $\vec{k}$ then $G_4(\vec{k}, \vec{r}; t)$ measures interparticle correlations weighted by the displacements along the vector $\vec{k}$. Particles which move in the direction perpendicular to $\vec{k}$ make a contribution to $G_4(\vec{k}, \vec{r}; t)$ which is the same as their contribution to the pair-correlation function $g(r)$. We notice that for $t>0$ four-point function $G_4(\vec{k}, \vec{r}; t)$ is not isotropic but depends on the angle $\theta$ between $\vec{r}$ and $\vec{k}$. Shown in the upper figure in Fig. 1 is the real part $G_4(\vec{k}, \vec{r}; t)$ for $T=0.45$ calculated at $t=\tau_\alpha$, and the lower figure shows the imaginary part. The maximum value of the real part of $G_4(\vec{k}, \vec{r}; \tau_\alpha)$ occurs for values of $\cos(\theta)$ corresponding to $\theta = 0°$ and $\theta = 180°$, which shows that the correlations are most pronounced for $\vec{r}$ parallel and antiparallel to $\vec{k}$. Thus, the correlations of the microscopic relaxation function is aniso-
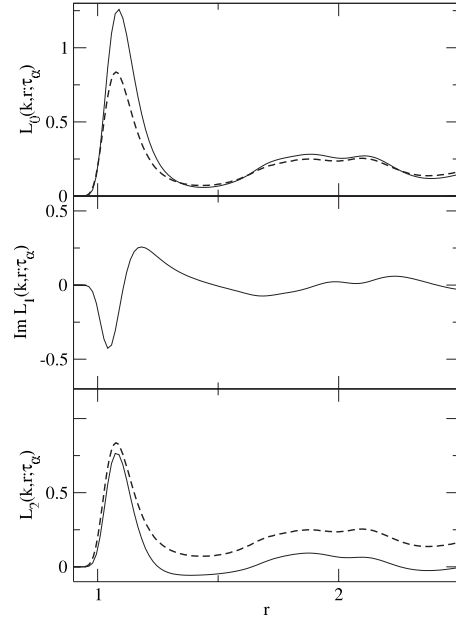


FIG. 2. The real part of $L_n(k, r; \tau_\alpha)$ for $n=0$ and 2 and the imaginary for $n=1$ for T=0.45 calculated at the $\alpha$ relaxation time. The dashed line in the figures is $g(r)e^{-2}$ where $g(r)$ is the pair-correlation function.

tropic on the $\alpha$ relaxation time scale and the correlations are the strongest when neighboring particles move in the same or in opposite directions.

To examine these anisotropic correlations at length scales around nearest-neighbor distances, we expand $G_4(\vec{k}, \vec{r}; t)$ into the Legendre polynomials

$$G_4(\vec{k}, \vec{r}; t) = \sum_n L_n(k, r; t) P_n(\hat{\vec{k}} \cdot \hat{\vec{r}}),$$

(12)

where $P_n$ is the $n$th Legendre polynomial, $\hat{\vec{k}} = \vec{k}/k$, $\hat{\vec{r}} = \vec{r}/r$, and

$$L_n(k, r; t) = \frac{2n+1}{4\pi} \int G_4(\vec{k}, \vec{r}; t) P_n(\hat{\vec{k}} \cdot \hat{\vec{r}}) d\hat{\vec{r}}.$$

(13)

If $G_4(\vec{k}, \vec{r}; t)$ does not depend on the angle between $\vec{k}$ and $\vec{r}$ then $L_n(k, r; t)$ is zero for all $n$ not equal to zero. Since there are nonzero real and imaginary parts to $G_4(\vec{k}, \vec{r}; t)$ for $t>0$ then there are nonzero real and imaginary parts to $L_n(k, r; t)$. By symmetry, the imaginary part is zero for even $n$, and the real part is zero for odd $n$.

Shown in Fig. 2 is the real part $L_n(k, r; \tau_\alpha)$ for $n=0$ and 2, and the imaginary part for $n=1$ at the alpha relaxation time $\tau_\alpha$ for $T=0.45$. There is a peak in $L_2(k, r; \tau_\alpha)$ and $L_0(k, r; \tau_\alpha)$ around the first peak of the pair-correlation function $g(r)$. The dashed lines in the figure are $g(r)e^{-2}$. Note that due to our definition of the $\alpha$ relaxation time $e^{-2}$ is the asymptotic limit of the isotropic component $L_0$ at $t = \tau_\alpha$, $\lim_{r \to \infty} L_0(k, r; \tau_\alpha) = F_s^2(k, \tau_\alpha) = e^{-2}$. The positive peak in $L_2(k, r; \tau_\alpha)$ indicates that particles that are initially separated by a distance corresponding to the first peak of $g(r)$ have a tendency to move in the same direction or in opposite directions, while the values close to zero around the first mini-
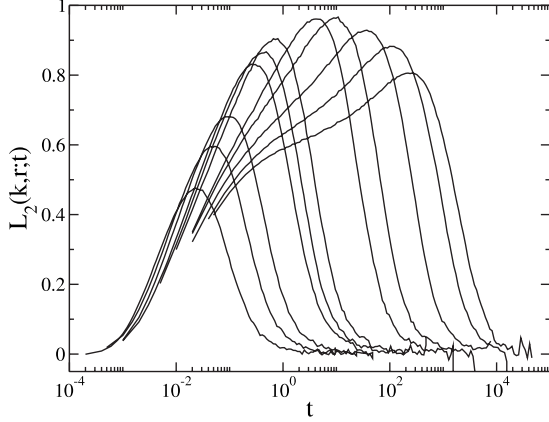
FIG. 3. The time dependence of the first peak of $L_2(k,r;\tau_\alpha)$ for $T=1.0$, 0.9, 0.8, 0.6, 0.55, 0.5, 0.47, and 0.45 shown from $l\epsilon$.

mum of the static structure factor can result from motion which is perpendicular to the initial separation vector. The spatial variation in the correlated motion on these length scales has been reported previously in colloidal suspensions [23] and is related to the breakup of the cage surrounding a particle.

The variation in the imaginary part of $L_1(k,r;\tau_\alpha)$ indicates that particles closer than the first peak of $g(r)$ are more likely to move apart, while particles at a distance greater than this peak are more likely to move closer together. In general, negative values of $L_1(k,r;t)$ indicate that particles move farther apart, while positive values indicate that particles move closer together. Similar conclusions were drawn by Weeks and Weitz [23] in their study of particles' rearrangements during cage breakdown and in the investigation of the dependence of the correlations between the motion of particles on their relative position [29].

To look at the time dependence of the anisotropy, we calculated the height of the first peak of $L_2(k,r;t)$ as a function of time, which is shown in Fig. 3 for $T=1.0$, 0.9, 0.8, 0.6, 0.55, 0.5, 0.47, and 0.45. The peak height starts at zero since the liquid is isotropic, then increases, reaches a maximum, and finally decreases to zero at long times. The height of the peak $\tau_{L2}$ is around the $\alpha$ relaxation time for high temperatures (Fig. 4), but its position increases slower with decreasing temperature than the $\alpha$ relaxation time and approximately follows the temperature dependence of the time corresponding to the peak position of the standard non-Gaussian parameter $\alpha_2(t)=3\langle\delta r^4(t)\rangle/[5\langle\delta r^2(t)\rangle^2]-1$, $\tau_{ng}$ (triangles in Fig. 4). Furthermore, the maximum value does not monotonically increase with a decrease in the temperature but rather reaches a maximum around $T=0.55$ then begins to decrease with decreasing temperature. Thus the anisotropy around nearest-neighbor distances initially increases upon supercooling the liquid but reaches a maximum and begins to slowly decrease when the liquid is cooled further. It is not known if the peak height continues to decrease or saturates at low temperatures.

## IV. FOUR-POINT STRUCTURE FACTOR $S_4(\vec{k},\vec{q};t)$

### A. Anisotropy of $S_4(\vec{k},\vec{q};t)$

To investigate the correlations between microscopic self-intermediate scattering functions at larger distances, we ex-
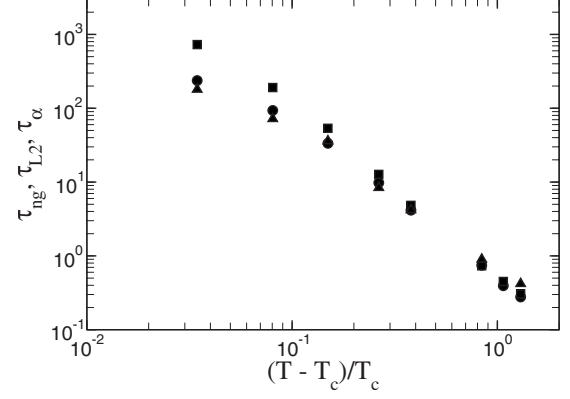


FIG. 4. The time at which the first peak of $L_2(k,r;t)$ reaches its maximum value $\tau_{L2}$ (squares) compared to the $\alpha$ relaxation time $\tau_\alpha$ (circles) and the peak time of the standard non-Gaussian parameter $\tau_{ng}$ (triangles).

amined the structure factor corresponding to $G_4(\vec{k},\vec{r};t)$,

$$S_4(\vec{k},\vec{q};t) = 1 + \frac{N}{V}H_4(\vec{k},\vec{q};t), \quad (14)$$

where $H_4(\vec{k},\vec{q};t)$ is the Fourier transform of $G_4(\vec{k},\vec{r};t)$ $-F_s^2(k;t)$. For $\vec{q}\neq 0$,

$$S_4(\vec{k},\vec{q};t) = \frac{1}{N}\sum_{n,m}\langle\hat{F}_n(\vec{k};t)\hat{F}_m(-\vec{k};t)e^{-i\vec{q}\cdot\vec{r}_{nm}(0)}\rangle. \quad (15)$$

Again, we fix $|\vec{k}|$ to be around the position of the first peak of the static structure factor for the $A$ particles $|\vec{k}|=7.25$.

Functions similar to Eq. (15) have been used to examine a growing dynamic length scale in glass forming liquids [4,9–11,16]. In Fig. 5 we show results similar to those presented in, e.g., Ref. [9]. Specifically, we show in $S_4(\vec{k},\vec{q}_\parallel;t)$ for $T=0.45$ at times $t=0$, $0.1\tau_\alpha$, $\tau_\alpha$, and $10\tau_\alpha$. Note that for $t=0$, $S_4(\vec{k},\vec{q};0)=S(q)$ where $S(q)$ is the static structure factor for the $A$ particles. We would like to emphasize that results shown in Fig. 5 are for one specific angle between $\vec{k}$ and $\vec{q}$; the angle between $\vec{q}$ and $\vec{k}$ is zero. It should be noted that for
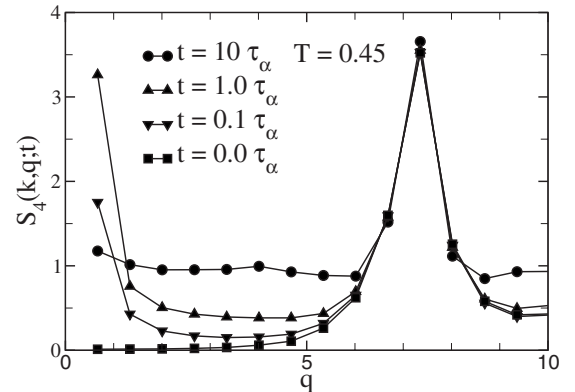


FIG. 5. The four-point correlation function $S_4(\vec{k},\vec{q};t)$ for $\theta=0$, where $\theta$ is the angle between $\vec{k}$ and $\vec{q}$ calculated at $t=0$, $0.1\,\tau_\alpha$, $\tau_\alpha$, and $10\tau_\alpha$ for a temperature $T=0.45$.
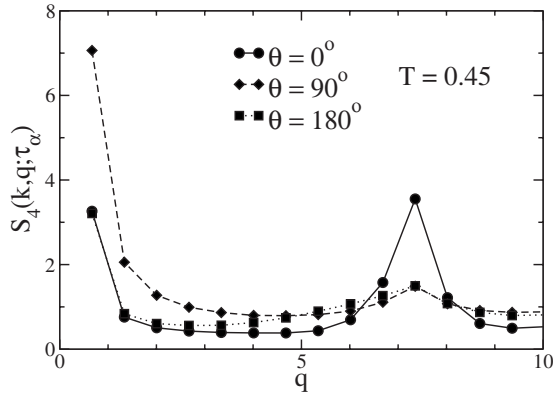
FIG. 6. The four-point correlation function $S_4(\vec{k}, \vec{q}; \tau_\alpha)$ for $\theta = 0°$, $90°$, and $180°$, where $\theta$ is the angle between $\vec{q}$ and $\vec{k}$ calculated for $T = 0.45$.

this angle between vectors $\vec{q}$ and $\vec{k}$, $S_4$ does not depend on time for $q=k$. This follows from definition (15); $S_4(\vec{k}, \vec{k}; t) = S(k)$ at all times.

The usual interpretation of results shown in Fig. 5 is that the increase of $S_4(\vec{k}, \vec{q}; t)$ at small $q$ values suggests a growing dynamic length scale $\xi(t)$. To find the dynamic length scale, it is common to fit the small $q$ behavior to a functional form and to examine the scaling of $S_4(\vec{k}, \vec{q}; t)$ for small $q$. In such a procedure, it is implicitly assumed that $S_4(\vec{k}, \vec{q}; t)$ is isotropic.

However, we find that $S_4(\vec{k}, \vec{q}; t)$ is not isotropic and depends on the angle between $\vec{k}$ and $\vec{q}$. Shown in Fig. 6 is $S_4(\vec{k}, \vec{q}, \tau_\alpha)$ for $T = 0.45$ and for $\theta = 0°$, $90°$, and $180°$ where $\theta$ is the angle between $\vec{k}$ and $\vec{q}$. The anisotropy of $S_4(\vec{k}, \vec{q}; t)$ adds a complication in finding a unique $\xi(t)$. The larger values of $S_4(\vec{k}, \vec{q}; t)$ for the smaller $\vec{q}$ values corresponding to $\theta = 90°$ suggest a longer length scale for atoms moving in the same direction than atoms moving in different directions. As we will see in Sec. IV C, this conclusion is consistent with the observed anisotropy of the dynamic correlation length.

Since we do not expect any slowly decaying with increasing distance spatial correlations between self-intermediate

scattering functions pertaining to different particles, we can safely assume that the $\vec{q} \to 0$ limit of $S_4(\vec{k}, \vec{q}; t)$ is well defined and it does not depend on the angle between vectors $\vec{q}$ and $\vec{k}$. However, the results shown in Fig. 6 suggest that the correlation length may be anisotropic. We should recall here that anisotropy in the correlated motion of particles on the $\beta$ relaxation time scale was concluded by Doliwa and Heuer [20]. We would like to emphasize that our results are consistent with an anisotropic dynamic correlation length but do not prove it. To conclusively prove such an anisotropy, one would need to simulate bigger systems in order to be able to examine the structure factor at smaller wave vectors $\vec{q}$.

We examine the anisotropy of the four-point structure factor by calculating the projection of $S_4(\vec{k}, \vec{q}; t)$ onto the Legendre polynomials,

$$I_n(k, q; t) = \frac{2n+1}{4\pi} \int S_4(\vec{k}, \vec{q}; t) P_n(\hat{\vec{k}} \cdot \hat{\vec{q}}) d\hat{\vec{q}}. \quad (16)$$

Shown in Fig. 7(a) is $I_0(k, q; \tau_\alpha)$ (i.e., the angular average of $S_4$) for $T = 1.0$, 0.8, 0.6, 0.55, and 0.45. In most simulational studies of four-point correlation functions, the correlation functions are shown as averages over different directions of wave vector $\vec{q}$; thus the results are similar to what is shown in Fig. 7(a). Note, however, that an average over different directions of $\vec{q}$ may not correspond to an angular average if the same number of wave vectors corresponding to each angle between $\vec{q}$ and $\vec{k}$ are not used in the average. Therefore, different routines to determine $S_4(\vec{k}, \vec{q}; t)$ can lead to different conclusions, and our results demonstrate that the averaging procedure needs to be performed with caution.

Shown in Fig. 7(b) is $I_2(k, q; \tau_\alpha)$ for $T = 1.0$, 0.8, 0.6, 0.55, and 0.45. The nonzero values of $I_2$ is a consequence of $S_4(\vec{k})$ being anisotropic on the $\alpha$ relaxation time scale. The anisotropy is largest for the smallest $q$ values. The temperature dependence of $I_2(k, q_0; \tau_\alpha)$ is shown as an inset to Fig. 7(b). The anisotropy at the $\alpha$ relaxation time for $q_0$ grows with decreasing temperature until around $T = 0.5$ then it remains approximately constant.
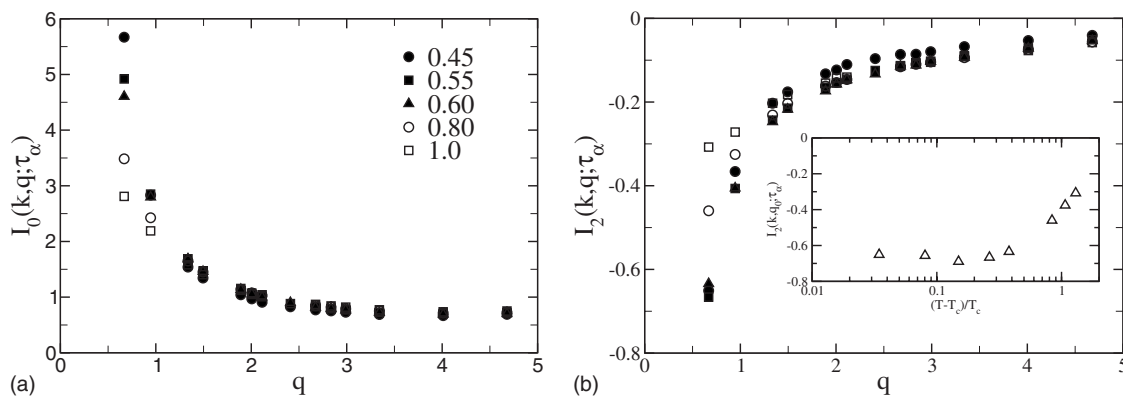


FIG. 7. The (a) projections $I_0(k, q; t)$ and (b) $I_2(k, q; t)$, as described in the text. The projection $I_0(k, q; t)$ is the average over angles $\theta$ between $\vec{k}$ and $\vec{q}$ of $S_4(\vec{k}, \vec{q}; t)$. If $S_4(\vec{k}, \vec{q}; t)$ does not depend on $\theta$ then $I_2(k, q; t)$ would be zero. Shown in the inset is $I_2(k, q_0; \tau_\alpha)$ where $q_0$ is the smallest wave vector allowed due to periodic boundary conditions as a function of temperature. The symbols in (a) and (b) correspond to the same temperatures.
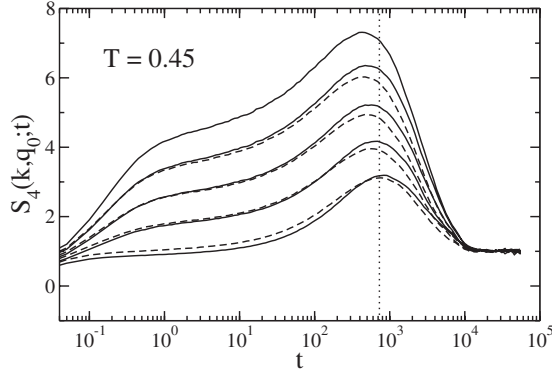
FIG. 8. Time dependence of $S_4(\vec{k}, \vec{q}_0; t)$ for different angles between $\vec{k}$ and $\vec{q}_0$ calculated for $T = 0.45$. The solid lines correspond to $\theta = 0°$, $30°$, $45°$, $60°$, and $90°$ listed from bottom to top. The dashed lines are $120°$, $135°$, $150°$, and $180°$ listed from top to bottom. The vertical dotted line indicates the $\alpha$ relaxation time.

## B. Time dependence of the anisotropy of $S_4(\vec{k}, \vec{q}_0; t)$

We now turn to the examination of the time dependence of the anisotropy of $S_4(\vec{k}, \vec{q}; t)$. To this end, we set $|\vec{q}|$ to be equal to the smallest wave vector allowed for our finite-size simulation box $|\vec{q}| = q_0 = 2\pi/L$ and calculate $S_4(\vec{k}, \vec{q}_0; t)$ as a function of time for different angles between $\vec{k}$ and $\vec{q}$. Results for $T = 0.45$ are shown in Fig. 8, and the vertical line marks the $\alpha$ relaxation time. We see that $S_4(\vec{k}, \vec{q}; t)$ grows with increasing time then reaches a maximum that depends on $\theta$ for a time around the $\alpha$ relaxation time and finally decays to one at long times. Note that while the position of the maximum is around the $\alpha$ relaxation time, the specific time at which the peak is reached depends on the angle between $\vec{k}$ and $\vec{q}$.

To determine the time dependence of the anisotropy, we examined $I_2(k, q_0; t)$ where $q_0$ is the smallest wave vector allowed due to periodic boundary condition $q_0 = 2\pi/L$. As seen in Fig. 9, $I_2(k, q_0; t)$ is zero at short and long times but develops a peak at intermediate times. Note that the shape of $I_2(k, q_0; t)$ is somewhat similar to that of $L_2(k, r_{peak}; t)$ shown in Fig. 3 except that $I_2(k, q_0; t)$ is negative [the last fact could be expected from the relation between $L_2(k, r; t)$ and $I_2(k, q; t)$]. The peak height increases with decreasing tem-
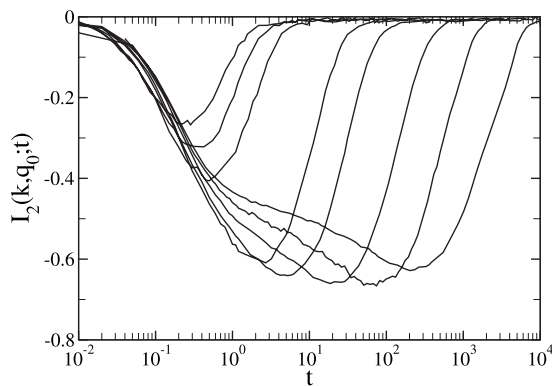


FIG. 9. Time dependence of $I_2(k, q_0; t)$ where $q_0$ is the smallest wave vector allowed due to periodic boundary conditions for $T = 1.0$, $0.9$, $0.8$, $0.6$, $0.55$, $0.5$, $0.47$, and $0.45$ listed from left to right.
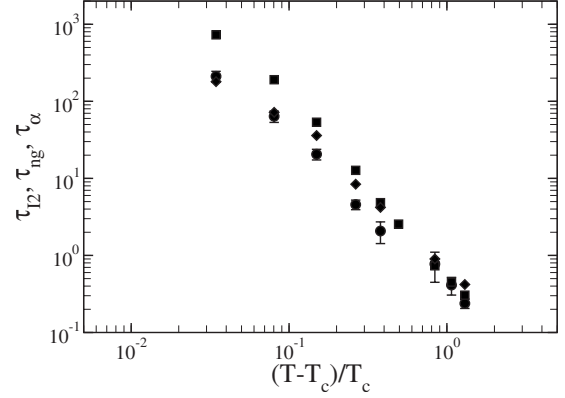


FIG. 10. The time corresponding to the maximum value of the magnitude of $I_2(k, q_0; t)$, $\tau_{I2}$, (circles) compared to the peak position of the non-Gaussian parameter $\tau_{ng}$ (diamonds) and the $\alpha$ relaxation time $\tau_\alpha$ (squares).

perature until $T = 0.47$, where it starts to decrease. However, as we show in the next subsection, the correlation lengths obtained from the fits at $T = 0.45$ are all close to or greater than half the box length, and it is currently unknown if the decrease in the peak height is a finite-size effect.

To determine when the anisotropy is a maximum at large distances, we found the time when $I_2(k, q_0; t)$ reaches its maximum value $\tau_{I2}$. Shown in Fig. 10 is the temperature dependence of $\tau_{I2}$ (circles) compared to $\tau_\alpha$ (squares) and the peak position of the standard non-Gaussian parameter $\tau_{ng}$ (diamonds). We notice similar trends as with the time corresponding to the maximum value of $L_2(k, r_{max}; t)$ in that the $\tau_{I2}$ occurs around $\tau_{ng}$ and has a similar temperature dependence.

### C. Effective dynamic correlation length

There has been some effort to determine the dynamic correlation length by fitting functions similar to $S_4(\vec{k}, \vec{q}; t)$ to different functional forms [9,11]. Lacevic et al. [9] used an Ornstein-Zernicke form $A/[1 + (\xi q)^2]$ to fit an overlap function $S_4^{ol}(q)$ that is isotropic by design, while Toninelli et al. [11] used $(A - C)/(1 + (\xi q)^\beta) + C$ to fit a function similar to the one studied in this work. Lacevic et al. found a correlation length growing with time until the peak time in the associated four-point susceptibility and then decreasing. In contrast, Toninelli et al. found a correlation length growing with time even after the peak in the associated susceptibility. It is possible that the difference between these findings was related to the presence of the new parameter $\beta$ in the fit used by Toninelli et al. More recently, Berthier et al. [6] used $A/[1 + (\xi q)^\beta]$ and found a value of $\beta = 2.4$ provided good fits to the same correlation function studied in the Ref. [6]. Here we focus on a possible anisotropy of the correlation length at the time equal to the $\alpha$ relaxation time and we leave its time dependence for a future study.

We started with

$$S_4(\vec{k}, \vec{q}; \tau_\alpha) = \frac{S_4(\vec{k}, 0; \tau_\alpha) - C}{1 + (\xi_\theta q)^2 + (aq)^4} + C, \quad (17)$$

as a fitting function to extract the dynamic correlation length $\xi_\theta$. In Eq. (17) we added a constant $C$ because of the growing
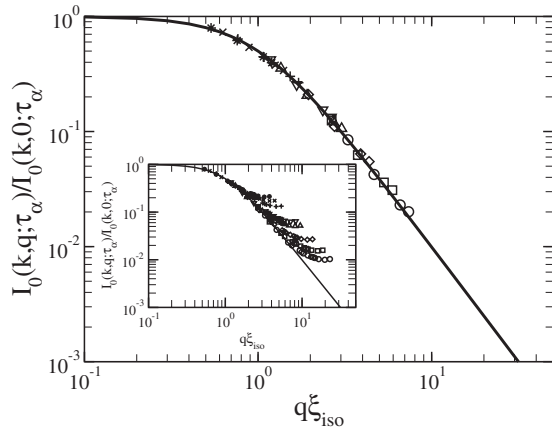
FIG. 11. The four smallest wave vectors allowed due to periodic boundary conditions of the projection $I_0(k,q;\tau_\alpha)/I_0(k,0;\tau_\alpha)$ versus $q\xi_{iso}$ for $T=0.45$, 0.47, 0.5, 0.55, 0.6, and 0.8. The solid line is the scaling function $1/(1+x^2)$. The inset shows all calculated wave vectors less than 5.

baseline which can be seen in Fig. 5. We note that since we do not expect any slowly decaying spatial correlations, in the limit $q\rightarrow0$, $S_4(\vec{k},\vec{q};\tau_\alpha)$ should be independent on the angle between $\vec{k}$ and $\vec{q}$. In contrast, in Eq. (17) we allowed for the dependence of the dynamic correlation length $\xi_\theta$ on the angle $\theta$ between $\vec{k}$ and $\vec{q}$. While fits to Eq. (17) were very good for $q<3$, the results were not satisfactory. The values of $S_4(\vec{k},0;t)$ were not consistent for different angles $\theta$ between $\vec{k}$ and $\vec{q}$ and the length scales $\xi_\theta$ obtained from the fits were greater than 40 at the lowest temperatures. To solve these problems, we performed the procedure described below. We emphasize that simulations of larger systems need to be performed to test this procedure and its results.

Initially, we attempted to set $C$ and $a$ to zero, thus fitting functions to the Ornstein-Zernicke form. We set $a$ to zero since it was always very small in the previously attempted fitting procedure. If this form is correct then one could ideally find $S_4(\vec{k},0;t)$ by fitting $S_4(\vec{k},\vec{q};t)$ for different angles between $\vec{k}$ and $\vec{q}$ under the condition that one obtains consistent results. We did not obtain consistent results for $S_4(\vec{k},0;t)$ with this procedure and also found that we needed to fix the value of $S_4(\vec{k},0;t)$ to obtain values of $\xi_\theta$ less than 50. To obtain an estimate for $S_4(\vec{k},0;t)$, we fit $I_0(k,q;t)$ for $q<1.5$ to an Ornstein-Zernicke form and then set the value of $S_4(\vec{k},0;t)=I_0(k,0;t)$ where $I_0(k,0,t)$ is obtained from the fits. Note that this is consistent with our assumption that the limit $\lim_{\vec{q}\rightarrow0}S_4(\vec{k},\vec{q};t)$ does not depend on the angle between $\vec{k}$ and $\vec{q}$.

If the glass transition is governed by a growing dynamic length scale then it is expected that for small enough $\vec{q}$ that $S_4(\vec{k},\vec{q};\tau_\alpha)/S_4(\vec{k},0;\tau_\alpha)$ versus $\xi q$ should be described by a universal function $F(q\xi)$ that is independent of temperature [7]. To check if this scaling holds for $I_0(k,q;\tau_\alpha)$, we plotted $I_0(k,q;\tau_\alpha)/I_0(k,0;\tau_\alpha)$ versus $q\xi_{iso}$ where $\xi_{iso}$ and $I_0(k,0;t)$ are obtained from the fits described above and the scaling function $1/(1+x^2)$, which is shown in Fig. 11. The subscript $iso$ in $\xi_{iso}$ emphasizes that this correlation length was ob-

tained from the orientational average $I_0(k,q;\tau_\alpha)$ of the four-point structure factor $S_4(\vec{k},\vec{q};\tau_\alpha)$. It appears that this scaling holds well for the small $q$ values, but we will again caution that simulations of larger systems need to be performed to verify this observation. Shown as the inset to the figure is $I_0(k,q;\tau_\alpha)/I_0(k,0;\tau_\alpha)$ versus $q\xi_{iso}$ for wave vectors with a magnitude less than five, and the deviation from the scaling behavior is obvious for the larger wave vectors. The correlation length obtained from $I_0(k,q;\tau_\alpha)$ is on the order of a particle diameter at the larger temperatures but grows to about five particle diameters at $T=0.45$. This growth of the correlation length is consistent with recent results of Berthier *et al.* [5]. Note, however, that at the lowest temperature $\xi_{iso}$ is comparable to the half the length of the simulation cell, which is the largest length we expect to be able to extract from the simulation without finite-size effects.

With the values of $S_4(\vec{k},0;\tau_\alpha)$ fixed using the fits from $I_0(\vec{k},0;\tau_\alpha)$, we fit $S_4(\vec{k},\vec{q};\tau_\alpha)$ where the angle $\theta$ between $\vec{k}$ and $\vec{q}$ are 0°, 45°, and 90° to an Ornstein-Zernicke form where only the correlation length is allowed to vary. We show $S_4(\vec{k},\vec{q};\tau_\alpha)/S_4(\vec{k},0;\tau_\alpha)$ versus $q\xi_\theta$, where $\xi_\theta$ depends on the angle $\theta$ between $\vec{k}$ and $\vec{q}$, for $T=0.8$, 0.6, 0.55, 0.5, 0.47, and 0.45 in Fig. 12. Only wave vectors with a magnitude less than 1.5 are shown, which corresponds to the four smallest wave vectors allowed due to periodic boundary conditions at each temperature and angle. The overlap is very good for the 18 functions shown and shown in the inset to Fig. 12 are the correlation lengths. They depend on the angle between $\vec{k}$ and $\vec{q}$, and the correlation lengths are largest for $\theta=90°$ and smallest for $\theta=0°$. Again, we observe that for $\theta=90°$, the correlation lengths are larger than half the simulation cell for $T=0.5$ (where $\xi_{90}\approx4.5$) and lower. This strongly suggests that already at $T=0.5$, simulations of larger systems are needed in order to verify the present results.

In previous studies it has been found that the correlation length is related to the $\alpha$ relaxation time according to a power law $\xi\sim\tau_\alpha^\gamma$ [6,9,30]. Recently, this behavior was rationalized by the inhomogeneous mode-coupling theory [7]. We fitted the correlation lengths to a power law of the form $a\tau_\alpha^\gamma$ and obtained values ranging from $\gamma=0.22\pm0.01$ for $\theta=0°$ and $\gamma=0.18\pm0.01$ for $\theta=90°$ (Fig. 9). Also shown in Fig. 9 is $\xi_{iso}$ obtained from $I_0(k,q;t)$; in this case we found $\gamma_0=0.21\pm0.01$, which is very close to the previously reported value of 0.22 [30]. Using this analysis, we find that the dynamic correlation length is not only different for different angles between $\vec{k}$ and $\vec{q}$, but they also grow at a different rate as the temperature is lowered and the $\alpha$ relaxation time increases. The range of correlations for particles moving in the same direction are longer than for particles moving in different directions, but it increases slower with decreasing temperature. The change in the correlation length is reminiscent of the crossover from stringlike regions to more compact regions discussed by Stevenson *et al.* [31]; but our simulations are not close enough to the glass transition to verify or refute this crossover.

Another scaling prediction is that $S_4(\vec{k},0;\tau_\alpha)\sim\tau_\alpha^\Delta$. To test this prediction, we fit $I_0(k,0;\tau_\alpha)$ to the form $a\tau_\alpha^\Delta$. In this way we obtain $\Delta\approx0.37$, which is again very close to the value of 0.4 reported in Ref. [30]. These values are slightly smaller
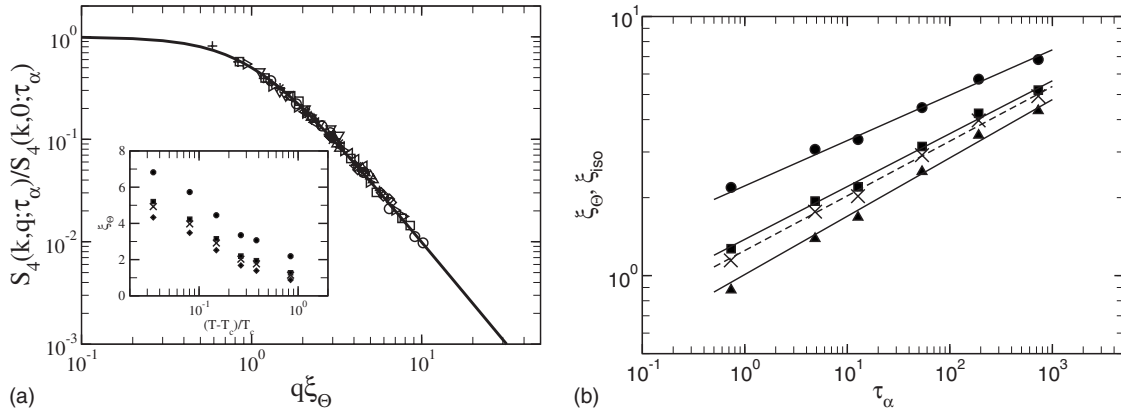
FIG. 12. (a) $S_4(\vec{k},\vec{q};t)/S_4(\vec{k},0;t)$ versus $q\xi_\theta$ for $\theta=0°$, 45°, and 90° where $\theta$ is the angle between $\vec{k}$ and $\vec{q}$ calculated for the temperatures $T=0.8$, 0.6, 0.55, 0.5, 0.47, and 0.45. The inset shows the length scales obtained from the different fits. (b) Dynamic correlation lengths versus the $\alpha$ relaxation time for $\theta=90°$ (circles), 45° (squares), and 0° (triangles). The solid lines are fits to $\xi\sim\tau_\alpha^\gamma$. The $X$'s and the dashed line correspond to $\xi_{iso}$ obtained from the fits of $I_0(k,q;\tau_\alpha)$.

than the recent inhomogeneous mode-coupling theory prediction of $\Delta=0.5$ [7].

## V. CONCLUSIONS

There have been many studies looking for a growing length scale that accompanies the drastic slowing down of the dynamics in supercooled and glass forming liquids. Recently, one such possibility was examined by Biroli *et al.* [32] where they associated a growing correlation length with a point-to-set correlation function in a model supercooled liquid. Ever since the observation of heterogeneous dynamics in supercooled and glassy systems, it has been suggested that a dynamic correlation length may be associated with the size of the dynamically heterogeneous regions. Since two-point correlation functions are inadequate to describe the correlated motion of atoms and correlated relaxation of the fluid, four-point correlation functions have been developed to examine this cooperative motion. Normally these correlation functions are assumed to be isotropic or are isotropic by design. However, it has been observed that correlated displacements of particles are not isotropic; thus it is not surprising that the four-point correlation functions might also not be isotropic.

In this work, we examined the anisotropy of a four-point correlation function. We found that for distances comparable to the nearest-neighbor distance, the anisotropy initially increases upon supercooling the liquid but then seems to saturate or even decrease at the lowest temperatures. The possible decrease suggests the possibility that the anisotropy is a transient feature only for mildly supercooled liquids. However, the decrease begins when we find that a dynamics correlation length, for $\theta=90°$, is around half the size of the simulation cell and thus it is possible that it is a finite-size effect. Furthermore, the time scale that this anisotropy is a maximum for nearest-neighbor distances is around the $\alpha$ re-

laxation time at higher temperatures but then it increases slower with decreasing temperature than the $\alpha$ relaxation time and roughly follows the time corresponding to the peak position of the non-Gaussian parameter $\alpha_2(t)$, $\tau_{ng}$.

For larger distances, we also found anisotropy of the four-point correlation function. We studied the time dependence of this longer ranged anisotropy and found that the time at which it is the largest also approximately follows $\tau_{ng}$ in the supercooled liquid. The longer-range anisotropy introduces a challenge in determining the growing dynamic length scale $\xi$ in glass forming systems. This difficulty is compounded by the relatively small system sizes usually employed in simulational studies of the glass transition. We developed a procedure to extract effective dynamic length scales, but larger system sizes need to be simulated to verify our results. Our procedure suggests that the dynamic correlation length is different depending on the relative direction of motion of two particles within the fluid. Furthermore, this anisotropic length scale also increases at a different rate with decreasing temperature.

We hope that our present work will stimulate future research in two different directions. First, we advocate the need to study larger systems and to perform serious finite-size analysis of the results [33–35]. In particular, we expect that in the small $\vec{q}$ limit, the four-point structure factor $S_4(\vec{k},\vec{q};t)$ is isotropic and we thus we expect its anisotropic component $I_2(k,q;t)$ to vanish in the small $\vec{q}$ limit. These expectations should be confirmed by simulations of larger systems. Second, we hope that this work will stimulate a development of a theoretical model that describes the anisotropy of four-point dynamic correlations.

## ACKNOWLEDGMENT

[1] M. Ediger, Annu. Rev. Phys. Chem. **51**, 99 (2000).

[2] R. Richert, J. Phys.: Condens. Matter **14**, R703 (2002).

[3] H. Andersen, Proc. Natl. Acad. Sci. U.S.A. **102**, 6686 (2005).

[4] L. Berthier, Phys. Rev. E **69**, 020201(R) (2004).

[5] L. Berthier and R. L. Jack, Phys. Rev. E **76**, 041509 (2007).

[6] L. Berthier, G. Biroli, J. Bouchaud, W. Kob, K. Miyazaki, and D. Reichman, J. Chem. Phys. **126**, 184503 (2007).

[7] G. Biroli, J. P. Bouchaud, K. Miyazaki, and D. R. Reichman, Phys. Rev. Lett. **97**, 195701 (2006).

[8] C. Donati, J. F. Douglas, W. Kob, S. J. Plimpton, P. H. Poole, and S. C. Glotzer, Phys. Rev. Lett. **80**, 2338 (1998).

[9] N. Lacevic, F. Starr, T. Schroder, and S. Glotzer, J. Chem. Phys. **119**, 7372 (2003).

[10] N. Lacevic, F. W. Starr, T. B. Schroder, V. N. Novikov, and S. C. Glotzer, Phys. Rev. E **66**, 030101(R) (2002).

[11] C. Toninelli, M. Wyart, L. Berthier, G. Biroli, and J. P. Bouchaud, Phys. Rev. E **71**, 041505 (2005).

[12] L. Berthier, G. Biroli, J. Bouchaud, L. Cipelletti, D. Masri, D. L'Hote, F. Ladieu, and M. Pierno, Science **310**, 1797 (2006).

[13] C. Dalle-Ferrier, C. Thibierge, C. Alba-Simionesco, L. Berthier, G. Biroli, J. P. Bouchaud, F. Ladieu, D. LHote, and G. Tarjus, Phys. Rev. E **76**, 041510 (2007).

[14] F. Lechenault, O. Dauchot, G. Biroli, and J. Bouchaud, EPL **83**, 46003 (2008).

[15] G. Biroli and J. Bouchaud, Europhys. Lett. **67**, 21 (2004).

[16] L. Berthier, G. Biroli, J. Bouchaud, W. Kob, K. Miyazaki, and D. Reichman, J. Chem. Phys. **126**, 184503 (2006).

[17] G. Szamel, Phys. Rev. Lett. **101**, 205701 (2008).

[18] M. Iwata and S. Sasa, EPL **77**, 50008 (2007).

[19] E. Flenner and G. Szamel, J. Phys.: Condens. Matter **19**, 205125 (2007).

[20] B. Doliwa and A. Heuer, Phys. Rev. E **61**, 6898 (2000).

[21] B. Doliwa and A. Heuer, Phys. Rev. Lett. **80**, 4915 (1998).

[22] Y. Gebremichael, M. Vogel, and S. Glotzer, J. Chem. Phys. **120**, 4415 (2004).

[23] E. R. Weeks and D. A. Weitz, Phys. Rev. Lett. **89**, 095704 (2002).

[24] W. Kob and H. C. Andersen, Phys. Rev. E **51**, 4626 (1995).

[25] W. Kob and H. C. Andersen, Phys. Rev. E **52**, 4134 (1995).

[26] S. E. Abraham and B. Bagchi, Phys. Rev. E **78**, 051501 (2008).

[27] T. Abete, A. de Candia, E. Del Gado, A. Fierro, and A. Coniglio, Phys. Rev. E **78**, 041404 (2008).

[28] In Ref. [10], both $g_4^{ol}$ defined in Eq. (8) and a more general collective version of this function were discussed.

[29] E. Weeks, J. Crocker, and D. Weitz, J. Phys.: Condens. Matter **19**, 205131 (2007).

[30] S. Whitelam, L. Berthier, and J. P. Garrahan, Phys. Rev. Lett. **92**, 185705 (2004).

[31] J. Stevenson, J. Schmalian, and P. Wolynes, Nat. Phys. **2**, 268 (2006).

[32] G. Biroli, J. Bouchaud, A. Cavagna, T. Grigera, and P. Verrochio, Nat. Phys. **4**, 771 (2008).

[33] L. Berthier, Phys. Rev. Lett. **91**, 055701 (2003).

[34] R. Stein, Ph.D. thesis, Stanford University, 2007.

[35] R. S. L. Stein and H. C. Andersen Phys. Rev. Lett. **101**, 267802 (2009).